

# The identification of physical close galaxy pairs

D.S.L. Soares

*Departamento de Física, ICEx, Universidade Federal de Minas Gerais, C.P. 702,  
30123-970 Belo Horizonte, MG Brazil*

dsoares@fisica.ufmg.br

## ABSTRACT

A classification scheme for close pairs of galaxies is proposed. The scheme is motivated by the fact that the majority of apparent close pairs are in fact wide pairs in three-dimensional space. This is demonstrated by means of numerical simulations of random samples of binary galaxies and the scrutiny of the resulting projected and spatial separation distributions.

Observational strategies for classifying close pairs according to the scheme are suggested. As a result, physical (i.e., bound and spatially) close pairs are identified.

*Subject headings:* galaxies: interactions — galaxies: kinematics and dynamics — galaxies: structure

## 1. Introduction

The investigation of binary galaxies is jeopardized by the intrinsic lack of temporal observational tracking of the orbital parameter space caused by orbital periods being of the order of hundreds of megayears. The alternative is the statistical study of samples of pairs relying on reasonable frequency distributions of the relevant orbital parameters. This has been done often since the pioneering work in the field by Holmberg (1937). Besides the unknowns mentioned above there is a second major setback: binary galaxy catalogues are always contaminated by the so-called optical pairs, i.e., unphysical, unbound pairs seen in projection on the plane of the sky. Earlier works, including Holmberg's, dealt with the problem by imposing restrictive selection criteria in the catalogues (e.g., Page et al. 1961; Karachentsev 1972, 1987; Turner 1976). Consequently the projected linear separations of pairs in these catalogues are typically 50 kpc. If one intends to study the distribution of galaxy mass to larger spatial extents such samples are clearly not adequate. A large sample of wide pairs is important in the determination of the size of dark halos, believed to exist within

and around the visible parts of galaxies. Later attempts have been made in this direction (van Moorsel 1982; Schweizer 1987; Soares 1989; Charlton & Salpeter 1991; Chengalur et al. 1993; Nordgren et al. 1998) with the addition of wide pairs with separations as large as 1 Mpc, and even more. The contamination by optical pairs remained a fundamental issue in all of these works.

Here I focus on a definite group of pairs, namely, close pairs, to investigate the important point, often neglected, that *closeness in the plane of the sky is not always a guarantee of three-dimensional closeness*.

An example from our backyard is useful as an illustration. Let us consider the most trivial galaxy pair: the Milky Way–Andromeda system (MW-And). Being the dominant galaxies in the Local Group, these galaxies form a wide pair with 700 kpc of separation. The cartoon in Figure 1 shows the MW-And pair and a line of sight pointing to the outskirts of the Virgo Cluster, located at about 15 Mpc. An observer at that location — assuming the Andromeda galaxy has the same linear dimension as the Milky Way — would notice a difference of less than 5% in their angular size. He could well classify the pair as a close one. With a velocity difference of  $119 \text{ km s}^{-1}$  at the line of sight considered, the MW-And pair would be a strong candidate to be in a list of close pairs. The reality is of another nature: MW-And is a wide pair. Its apogalacticon separation might be estimated at about 2 Mpc, if the system is on a highly-eccentric orbit and the galaxies have approximately  $10^{12} M_{\odot}$ . Most plausible, the system has recently reached its apocentric configuration in a slightly-eccentric orbit, implying a significant transverse velocity at present. The proper motion of M31 has indeed been constrained to about  $100 \text{ km s}^{-1}$  by Loeb et al. (2005).

# MILKY WAY–ANDROMEDA

as a close pair

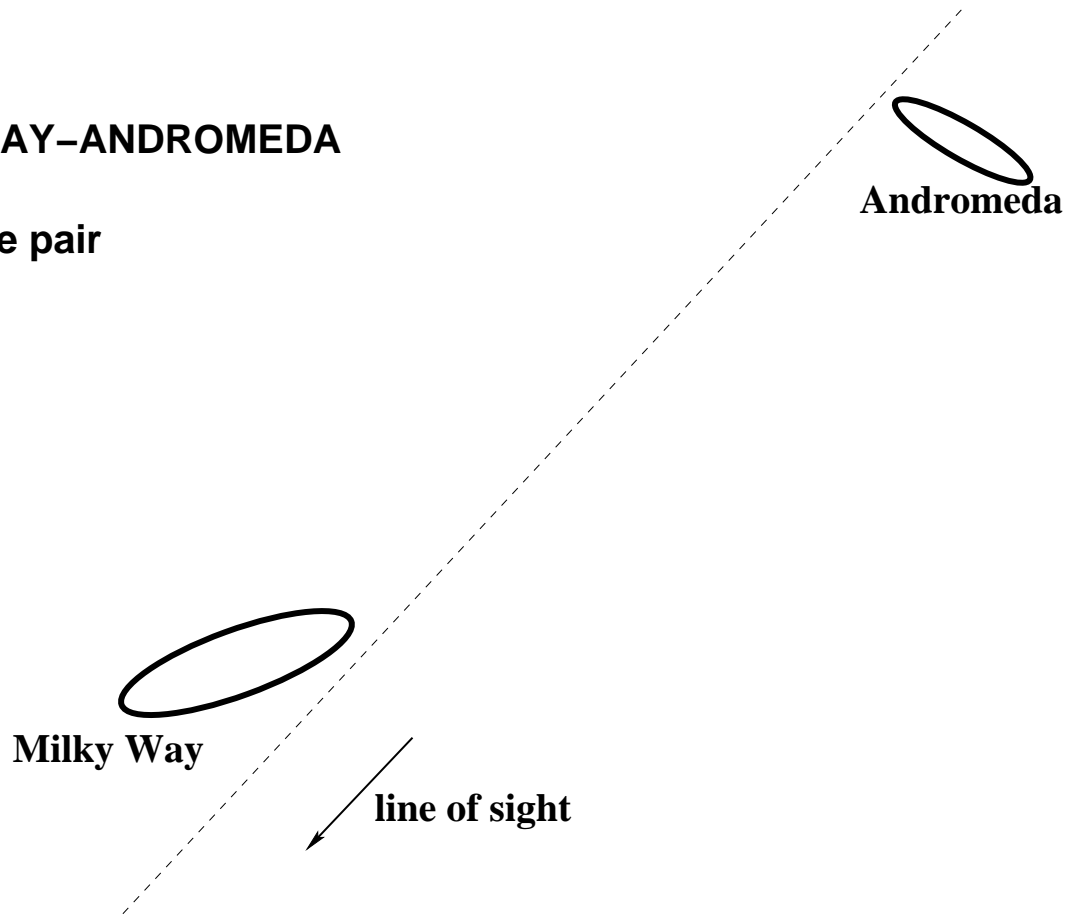


Fig. 1.— MW-And system and a line of sight towards a hypothetical distant observer.

Recent papers aimed at investigating a number of properties of close pairs, such as star formation (Barton et al. 2000; Woods et al. 2006) and merger rates, do not give due relevance to the fact that projected physical separation ( $R_p$ ) cannot suffice as a unique constraint for closeness. Patton et al. (2000, 2002) define a close pair as having  $5h^{-1} < R_p \leq 20h^{-1}$  kpc and an upper limit in the pair radial-velocity difference of  $500 \text{ km s}^{-1}$ . The velocity criterion represents a somewhat loose general constraint on physical association. They are followed by others in essentially the same procedure (e.g., Nikolic et al. 2004). I argue here that this is just the first step in the selection procedure. It has to be complemented by an investigation of the tidal effects on the individual galaxies in the pair in order to have a clear definition of closeness.

Other studies address the presence of Markarian activity in galaxy pairs. Byrd & Valtonen (2001) find that Markarian activity is an indication of tidal interaction. Their results should be confronted with the closeness of the sample pairs identified by an activity-blind procedure, as suggested here.

In section 2 I show, using Monte Carlo simulations, that a small projected separation is not a secure and fair indication of a small spatial separation. This is a consequence of the fact that two-body orbits have most of their phase-space time at apocentric configurations (cf. Kepler’s law). The scene is thus set for the presentation of the classification scheme in section 3. The relevant observational data for sorting apparently close pairs throughout classes are suggested in section 4.

Section 5 summarizes the main conclusions.

## 2. Spatial and projected separations in close pairs

The most simple way of disclosing the three-dimensionality of projected separations in binary galaxies is by means of Monte Carlo-type simulations of bound pairs. These are generally an useful tool when one wants to analyze an observed binary sample in order to extract information such as galaxy mass and angular momentum and orbital period and eccentricity. Such a statistical method has been used intensively in the past (e.g., Turner 1976; van Moorsel 1982; Schweizer 1987; Oosterloo 1988; Soares 1990, 1996).

To simulate a sample of binary galaxies a number of input orbital parameters have to be specified, namely, the distribution of spatial separations and of orbital eccentricities. Furthermore, a mass model for galaxies has to be defined, as do projection rules to transform orbital velocity and radial separation into observed quantities such as line-of-sight velocity difference and apparent projected separation.

## 2.1. Simulation procedure

The simulation procedure is established according to the objective one has in mind. Here the main goal is to investigate how close pairs, defined by their apparent separations, are distributed in three dimensions or, in other words, are distributed in the apparent versus spatial separation plane. The simulations are case problems that span a wide range of possibilities in the whole phase-space of binary orbits. To reach the goal I generated samples of 2000 artificial pairs with the following specifications.

- (i) Mass model: two equal-mass galaxies in Keplerian orbits. Galaxies move under their mutual point-mass Newtonian gravitational potential. I further add the restriction that galaxies never get closer than the sum of their (approximate) half-mass radii. I adopt a conservative value of 10 kpc for the sum. In practice this means that galaxies getting closer than this limiting separation rapidly merge and are therefore excluded from the simulated sample. Self-consistent  $N$ -body simulations of binary-galaxy orbit secular evolution have conclusively shown that such systems indeed merge on a time-scale much smaller than a Hubble time (e.g., Bartlett & Charlton 1995; Chan & Junqueira 2001). Evidently, galaxies are not point masses and may possess well-extended (dark) mass distributions. As long as the binary system is isolated from a third-body gravitational influence, and furthermore the mutual gravitational interaction is only radially dependent, the point-mass assumption is a reasonable description of the general consequences of orbital angular momentum conservation, which relies on Kepler’s areal law, i.e., on the fact that galaxies spend most of their time at apocenter.
- (ii) Spatial separation: samples with either a fixed apocentric separation  $R_{apo}$  of either 200 or 600 kpc. These two values span fairly the average (apocentric) separations of binary galaxies as suggested by several works (Soares 1989; Schweizer 1987; Charlton & Salpeter 1991; Chengalur 1994; Nordgren 1997). A more rigorous simulation should consider a distribution of binary spatial separations. Earlier work (Gott & Turner 1979, but see Soares 1989, p. 17) suggested that binary galaxies follow, down to small scales, an extension of the classical galaxy two-point correlation function (Peebles 1980), but more recent evidence points to a multi-variable correlation function, depending on galaxy type, luminosity and local galaxy number density. An  $R_{apo}$  value smaller than 200 kpc is not considered here because, as mentioned above, such pairs merge quickly.
- (iii) Eccentricity distribution: three distributions, spanning the entire orbital phase-space. They are  $f(e) = \delta(0.9)$ ,  $f(e) = 2e$ , and  $f(e) = \delta(0)$ . If binary galaxies were formed by early capture, suggested already by Holmberg (1937; see also Schweizer 1987), the triangular distribution  $f(e) = 2e$  would be suitable since it allows for some amount of

transverse orbital motion. The extreme cases of highly eccentric orbits ( $e = 0.9$ ) and circular orbits bracket the triangular distribution and are considered for completeness and reveal fruitful consequences (see below).

- (iv) Projection on the sky: the normal to the orbital plane is distributed at random *in space*, that is, the orbital inclination  $i$  has a distribution  $f(i) \propto \sin(i)$ .

A pair orbit is simulated with prescriptions 1–4; velocities and radial separations are drawn at a random time instant within the orbit, and, from prescription 4, the projected separation onto the plane of the sky and the corresponding line-of-sight pair velocity difference are calculated. The random choice of orbital phase implies, from Kepler’s law, that pairs at apocenter — large separations — are naturally favored. For each pair of  $R_{apo}$  and  $f(e)$  the process is repeated until a list of 2000 pairs is simulated, and therefrom I investigate the correlation between projected and spatial separation.

## 2.2. Projected versus spatial separation

A *putative* close pair is defined as a pair of galaxies having at most the fiducial projected separation  $R_{p,max} = 50$  kpc, which is typical in the studies mentioned above. I then ask: *How many pairs with  $R_p \leq R_{p,max}$  have spatial separations  $R > R_{p,max}$ ?*

Figure 2 shows  $N - R_p$  histograms for the two cases considered here,  $R_{apo} = 200$  and 600 kpc, and for the three distributions of eccentricities,  $f(e) = \delta(0.9)$ ,  $f(e) = 2e$  and  $f(e) = \delta(0)$ . Shaded areas represent close pairs as defined above. Sample median values of  $R_p$  are shown in the figure and in Table 1. As expected, the least median  $R_p$  occurs for  $f(e) = \delta(0.9)$  and for the triangular distribution  $f(e) = 2e$ , being essentially the same for both distributions. It amounts to 60% of  $R_{apo}$ , meaning about 120 and 360 kpc respectively. In the simulations of pairs in circular orbits, the median  $R_p$  is exactly 87% of  $R_{apo}$ . It can be noted from Fig.

Table 1: Number of simulated close pairs out of 2000

$R_{apo}$	$f(e) = \delta(0.9)$	$f(e) = 2e$	$f(e) = \delta(0)$
	Median $R_p$	Median $R_p$	Median $R_p$
200 kpc	284	228	51
	121 kpc	125 kpc	173 kpc
600 kpc	67	30	4
	360 kpc	360 kpc	520 kpc

2 that the  $R_p$  distributions are the same irrespective of  $R_{apo}$  for all eccentricities. Such an overall behavior is expected due to self-similarity, since the dynamical problem is the same — the sole difference on the orbit length scale. There is a slight fluctuation, however, in the triangular eccentricity distribution case (Fig. 2, *middle panels*), which is due to the additional degree of freedom introduced by the random choice of the pair eccentricity. But even here  $R_p$  distributions are the same, with a noticeable decrease of pairs at small projected separations as compared to the high-eccentricity simulations (Fig. 2, *top panels*).

The important difference between the distributions with  $R_{apo} = 200$  and 600 kpc is the percentage of close pairs ( $R_p \leq 50$  kpc). According to Table 1, 14% of the total population of pairs with  $f(e) = \delta(0.9)$  and  $R_{apo} = 200$  kpc are close pairs, a figure that decreases to 3% if  $R_{apo} = 600$  kpc. This is a ready consequence of the much wider phase space available for pairs with the larger  $R_{apo}$ .

As seen above, all simulations have large median  $R_p$ , even greater than  $2 \times R_{p,max}$ , which shows that at least half of simulated pairs have spatial separations much greater than  $R_{p,max}$ . This is further confirmed by the data shown in Table 2, which represent the most important result, as far as the classification of close pairs is concerned: more than half of the simulated pairs with  $R_p \leq 50$  kpc have three-dimensional separations greater than 50 kpc.

If real binaries are predominantly in circular orbits, 100% of pairs have — from input — spatial separation of  $R > 50$  kpc, and close pairs are thus very few, less than 3% of the simulated population. The firm conclusion from these results is that apparent separations are not bona-fide indicators of spatial closeness. Close pairs with  $R_{apo} < 200$  kpc, not included in the simulations, would not substantially alter the conclusion.

In the next section, a classification scheme is put forward whose main purpose is to discriminate close pairs against their *real* physical dynamical character. The classification is a pre-requisite for any further astrophysical investigation of the properties of galaxies in close pairs.

Table 2: Percentage of close pairs with  $R > 50$  kpc

$R_{apo}$	$f(e) = \delta(0.9)$	$f(e) = 2e$	$f(e) = \delta(0)$
200 kpc	52.5%	69.3%	100%
600 kpc	53.7%	73.3%	100%

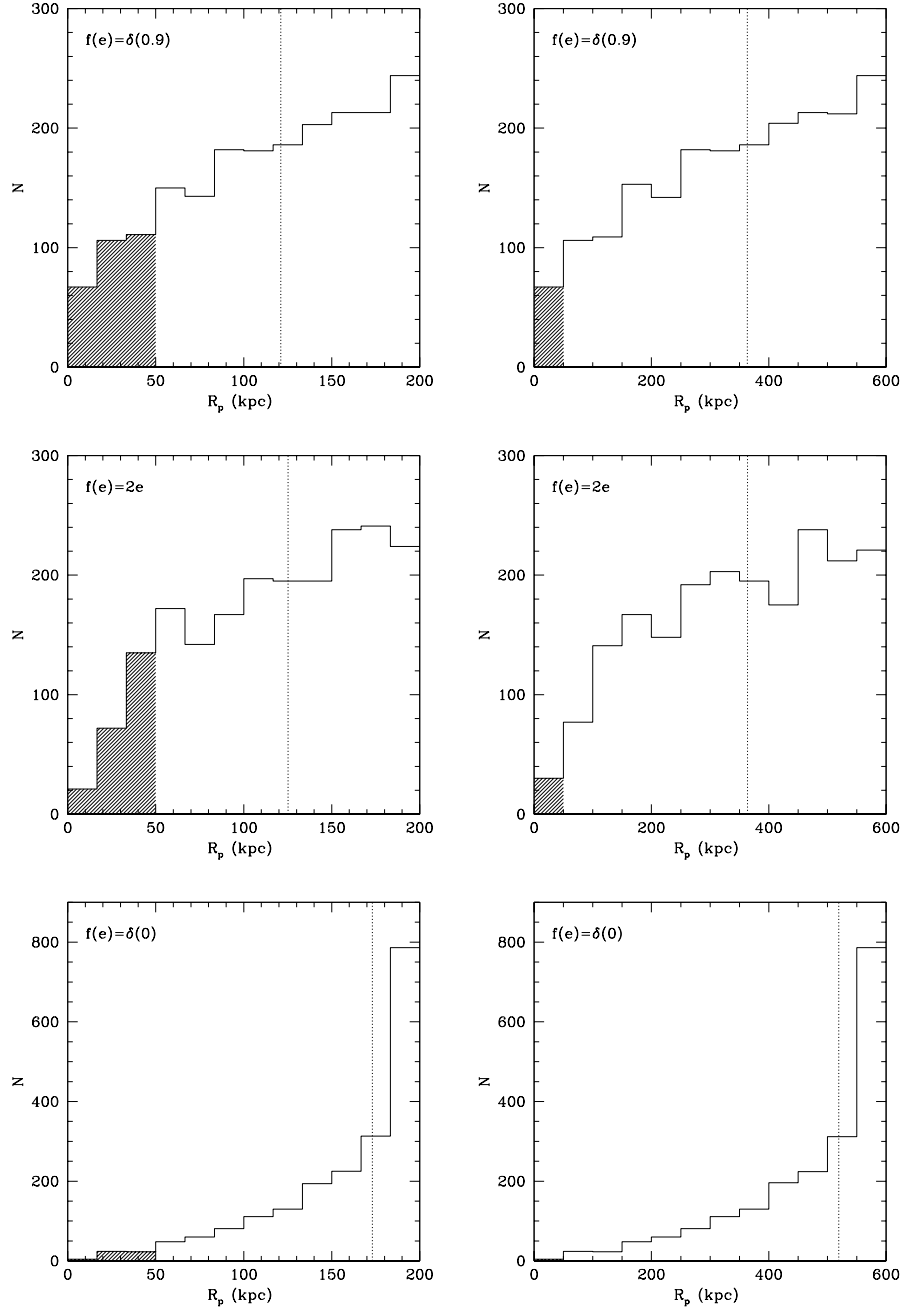


Fig. 2.— Distribution of projected separations  $R_p$  for simulated pairs, with different eccentricity distributions  $f(e)$  and apocentric separation  $R_{apo}$ . *Left:*  $R_{apo} = 200$  kpc. *Right:*  $R_{apo} = 600$  kpc. Dotted vertical line in all panels marks each sample’s median  $R_p$ . Shaded areas show the close-pair population.

### 3. The classification scheme

The ground property in the classification scheme is the strength of tidal interaction between pair galaxies. Table 3 shows the four suggested classes of close pairs. The main goal is clearly discriminating between pairs that are interacting through tidal forces and those whose galaxies do not have their internal structure substantially affected by the mutual differential gravitational interaction. The strength of tidal activity between two extended mass distributions, with centers of mass separated by  $R$  is — grossly speaking — inversely proportional to  $R^3$ , thus justifying the consideration of tidal activity as the crucial property for a classification scheme. As seen in Table 3, types CP I — mergers — and CP IV — unphysical pairs — are extreme types. Type I pairs are evolved type II pairs, and type IV pairs are misclassified close pairs, i.e., optical pairs.

Any study of the effects of closeness on the properties of galaxy pairs must be preceded by an observational selection procedure in order to classify the sample under study into the four classes. In the next section suggestions for the required observational programs are given.

## 4. Observational strategy for classifying close pairs

### 4.1. CP I and CP IV

The CP I types are easily sorted by looking to their optical disturbed morphology. Individual galaxies are hardly seen as separate entities. The CP IV types, on the other hand, are selected by their discordant redshifts. A very conservative lower limit to the line-of-sight galaxy velocity difference in the pair of  $300 \text{ km s}^{-1}$  may be adopted as an initial guess to distinguish optical pairs. This limit corresponds to the relative velocity of two  $10^{12} M_{\odot}$  (visible plus dark) galaxies on a circular orbit whose centers of mass are separated by 100 kpc. A detailed study of redshift asymmetries in the pair sample under investigation

Table 3: Classification of close pairs

Class	Pair	Interaction
CP I	merger	strongest
CP II	tide-loud	strong
CP III	tide-quiet	weak
CP IV	optical	weakest

might be used in order to evaluate the contamination by optical companions. Valtonen & Byrd (1986) find that physical pairs exhibit an equal number of positive or negative redshifts relative to the primary while that is not true for non physical optical pairs.

The most difficult types to classify are CP II and CP III, which require a specially suitable observational strategy that takes into account the kinematical consequences of tidal forces.

## 4.2. Tidal kinematics

A straight application of the impulse approximation (Binney & Tremaine 1987) for tidal effects in high-speed encounters (“fly-bys”) of extended objects leads to symmetrical perturbations. That is, two test particles, at symmetric positions with respect to the perturbed object center, acquire velocity increments of the same magnitude and opposite direction (Binney & Tremaine, eq. [7-54], p. 438). This will result in symmetric velocity profiles. A perturbed disk galaxy would thus exhibit no signature of tidal forces in its rotational profile.

Although the impulse approximation has been successfully shown to be consistent with numerical experiments for mass and energy exchanges between interacting spherical galaxies (Aguilar & White 1985), it does not hold here. Bound pairs are mid way between the fly-by encounters in which the impulse approximation does apply and pairs that are quickly evolving through a merger phase. Concerning the latter case, Mihos et al. (1998) made an  $N$ -body merger model of NGC 7252, a galaxy with conspicuous tidal tails. The initial pre-merger galaxies have symmetrical rotation curves that evolve along the merger process to a final asymmetrical velocity profile (see their Fig. 6). Hence, one expects that at perigalacticon bound pairs will show slightly — but noticeably — distorted velocity profiles before they ultimately enter a merging phase.

Furthermore, Barton et al. (1999) have shown, using  $N$ -body simulations of galaxy encounters, that tidal interactions induce noticeable distortions on the rotation curves of spiral galaxy models (see their Fig. 1).

The asymmetry of the velocity profile of both galaxies at closest approach will be used here as an indication of *strong* — loud — tidal forces, therefore implying spatial proximity. This is the rationale underlying the discussion of the kinematics of CP II and CP III classes below.

### 4.3. CP II and CP III

The most confident criteria for CP II and CP III classification are: (1) broadband photometry, (2) kinematics from optical single-slit spectroscopy, and (3) global H I spectral line low-resolution velocity profiles. These are intentionally designed to be low cost procedures for the classification. Strong tidal forces affect the outcome of all three sorts of observations. Ideally, all three should be used, as, for example, in Marziani et al. (1999). They studied the close pair UGC 3995A+B (CPG 140, in Karachentsev 1972, 1987), whose POSS-II *B*-band image is shown in Fig. 3.

Galaxy centers are separated by approximately  $30''$ , and the smaller component B is seen in front of the spiral disk of component A. Marziani et al. (1999) proceeded to broadband photometry decomposition and found unperturbed individual solutions for both galaxies. Optical spectroscopy reveals symmetrical kinematics relative to the galaxy centers. That is, the rotation-curve amplitudes are the same on the receding and approaching sides of both galaxies. The H I global profile is symmetrical as well. The optical velocity difference is  $20 \text{ km s}^{-1}$  (internal error of  $18 \text{ km s}^{-1}$ ), and the H I velocity difference is  $1 \text{ km s}^{-1}$ , from Sulentic & Arp (1983). These observations suggest that the pair is a CP III, a “tide-quiet” close pair, seen at or close to apocentric orbital phase, near turnover. It is worthwhile mentioning that the orbital interpretation above diverges from Marziani et al. They claim that the pair is seen either before or after their closest approach. This seems unlikely, however because in this case tidal perturbations would be evident in the observations. The classification scheme relies on the assumption that tidal activity impresses asymmetrical signatures on morphology and kinematics.

A counterexample to UGC 3995, namely, a “tide-loud” close pair, is SBG 249 (Soares et al. 1995). Long-slit spectroscopy has been performed and analyzed by Carvalho & Soares (2007, in preparation). The galaxies are NGC 1738 (eso-lv 5520490) and NGC 1739 (eso-lv 5520500). They have partially overlapped disks. Two spectra were obtained with the Double Spectrograph instrument mounted at the Palomar 5 m telescope, on 1998 February 27–28. Figure 4 shows an isophote map of the pair, with the  $128''$  long slits superposed. The derived rotation curves are shown in Fig. 5 (both figures from Carvalho & Soares 2007, in preparation).

The asymmetry is apparent in NGC 1738 and hinted at in NGC 1739. The southwestern side of NGC 1738 rotates almost twice as much as the northeastern side; that is, its closest side to NGC 1739 rotates at a greater speed than the farthest side. The northwestern side of NGC 1739 flattens out at about  $100 \text{ km s}^{-1}$ , while the southeastern side seems to be rising up at the last measured point. It is clear that the rotation profiles are strongly affected by their mutual tidal influence. On the other hand, the spectrum of the overlapped portion of



Fig. 3.— *B*-band image from the POSS-II Digital Sky Survey of the close pair UGC 3995A+B. The smaller galaxy B is seen in front of the disk of the larger component. See also Marziani et al. (1999). North is up, and east is left.

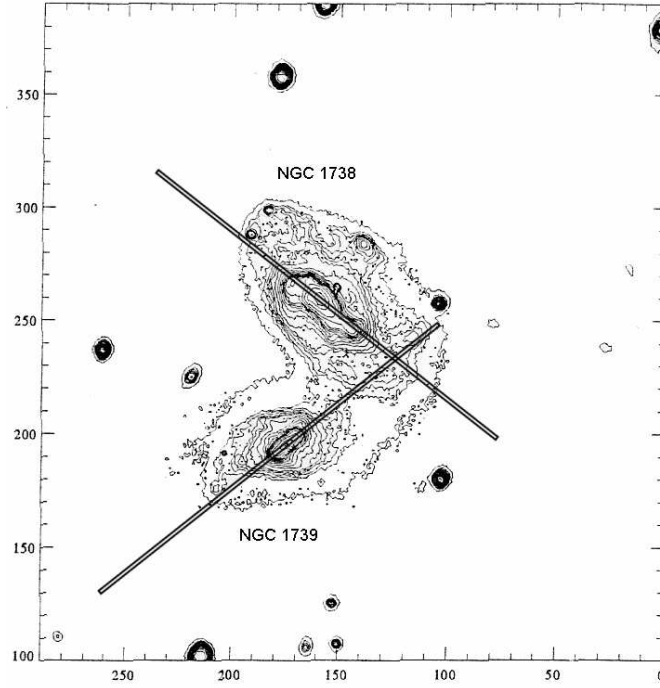


Fig. 4.— *R*-band isophote map of SBG 249 from Carvalho & Soares (2007, in preparation). NGC 1738 (ESO-LV 552490) is the background galaxy. Slits are  $128''$  long. North is up, and east is left.

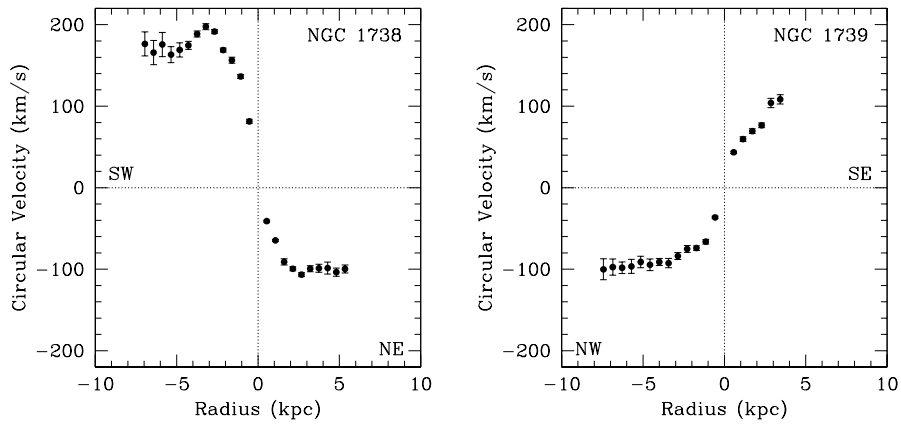


Fig. 5.— Rotation curve of NGC 1738 (*left*) and NGC 1739 (Carvalho & Soares 2007, in preparation). The southwestern side (SW) of the NGC 1738 disk and the northwestern side (NW) of NGC 1739 are partly overlapped.

the system is clearly disentangled showing that both disks rotate quite independently and, as can be seen in Fig. 5, in opposite directions. This also rules out classification as a CP I, in spite of the disturbed morphological appearance of the pair.

The line of sight velocity difference is  $60 \text{ km s}^{-1}$  (internal error of  $20 \text{ km s}^{-1}$ ). Since they are low-mass galaxies, this is consistent with SBG 249 being a CP II seen at or close to perigalacticon in an eccentric orbit (cf. the Appendix in Soares 1996). Additional broadband photometry and global H I observation are planned for the pair.

The strength of the asymmetry in the velocity profile might depend on the disk rotation sense relative to the orbit sense. Howard et al. (1993) performed detailed simulations of tidally induced structures in disk galaxies. They discuss morphological disturbances and find that retrograde encounters are less effective in producing disturbances. If the result applies also to kinematical disturbances then pairs that pass close enough to be CP II — tide-loud pairs — might resemble CP III types if the galaxy’s rotation sense is opposite to the orbit sense. These cases require careful analysis of *both* broadband photometry and pair kinematics as was the case for CPG 140 discussed above.

## 5. Conclusion

Monte Carlo simulations of close pairs of galaxies show that a projected separation restrictive criterion does not guarantee closeness in space. Accordingly, a simple classification scheme of close pairs is proposed and an observational strategy is suggested for sorting out a sample before any kind of astrophysical investigation of their properties is made. The classification is based on kinematical and dynamical criteria and on the pair’s overall morphological appearance. The required observations are thus broadband photometry and optical and H I 21-cm line spectroscopy. The latter is of course only suitable for pairs with late-type galaxies.

For a sample of close pairs, defined initially by their closeness in the plane of sky, the three kinds of observations are sufficient in ascribing to each pair one of the classes suggested. Classes are defined by the strength of present tidal activity and optical morphology. They are mergers (CP I), tide-loud pairs (CP II), tide-quiet pairs (CP III), and physically unbound optical pairs (CP IV).

I thank David Balparda de Carvalho for helpful discussions on the close-pair subject and for a careful reading of the manuscript. The anonymous referee is gratefully acknowledged for useful comments and suggestions to improve the text. The Second Palomar Observatory Sky

Survey was made by the California Institute of Technology with funds from the National Science Foundation, the National Geographic Society, the Sloan Foundation, the Samuel Oschin Foundation, and the Eastman Kodak Corporation. I thank the Brazilian agency FAPEMIG for partial support.

## REFERENCES

- Aguilar, L.A., & White, S.D.M. 1985, *ApJ*, 295, 374
- Bartlett, R.E., & Charlton, J.C. 1995, *ApJ*, 449, 447
- Barton, E.J., Bromley, B.C., & Geller, M.J., 1999, *ApJ*, 511, L25
- Barton, E.J., Geller, M.J., & Kenyon, S.J., 2000, *ApJ*, 530, 660
- Binney, J., & Tremaine, S. 1987, *Galactic Dynamics*, (Princeton: Princeton University Press)
- Byrd, G., & Valtonen, M.J. 2001, *AJ*, 121, 2943
- Chan, R., & Junqueira, S. 2001, *A&A*, 366, 418
- Charlton, J.C., & Salpeter, E.E. 1991, *ApJ*, 375, 517
- Chengalur, J.N. 1994, PhD thesis, Cornell University
- Chengalur, J.N., Salpeter, E.E., & Terzian, Y. 1993, *ApJ*, 419, 30
- Goth, J.R., & Turner, E.L. 1979, *ApJ*, 232, L79
- Holmberg, E. 1937, *Annals Obs. Lund*, 6, 1
- Howard, S., Keel, W.C., Byrd, G., & Burkey, J. 1993, *ApJ*, 417, 502
- Karachentsev, I. 1972, *Soob. Sp. Astr. Obs. Akad. Nauk.*, 7
- Karachentsev, I. 1987, *Double Galaxies* (Moskow: Nauka), in Russian
- Loeb, A., Reid, M.J., Brunthaler, A., & Falcke, H. 2005, *ApJ*, 633, 894
- Marziani, P., D’Onofrio, M., Dultzin-Hacyan, D., & Sulentic, J.W. 1999, *AJ*, 117, 2736
- Mihos, J.C., Dubinski, J., & Hernquist, L. 1998, *ApJ*, 494, 183
- van Moorsel, G.A. 1982, PhD thesis, University of Groningen

- Nordgren, T.E. 1997, PhD thesis, Cornell University
- Nordgren, T.E., Chengalur, J.N., Salpeter, E.E., & Terzian, Y. 1993, ApJS, 115, 43
- Nikolic, B., Cullen, H., & Alexander, P. 2004, MNRAS, 355, 874
- Oosterloo, T.A. 1988, PhD thesis, University of Groningen
- Page, T., Dahn, C.C., & Morrison, F.F. 1961, AJ, 66, 614
- Patton, D.R., Carlberg, R.G., Marzke, R.O., et al. 2000, ApJ, 536, 153
- Patton, D.R., Pritchet, C.J., Carlberg, R.G., et al. 2002, ApJ, 565, 208
- Peebles, P.J.E. 1980, The Large-Scale Structure of the Universe (Princeton: Princeton University Press)
- Schweizer, L.Y. 1987, ApJS, 64, 427
- Soares, D.S.L. 1989, PhD thesis, University of Groningen
- Soares, D.S.L. 1990, A&A, 238, 50
- Soares D.S.L., de Souza R.E., de Carvalho R.R., & Couto da Silva T.C. 1995, A&AS, 110, 371
- Soares, D.S.L. 1996, A&A, 313, 347
- Sulentic, J.W., & Arp, H. 1983, AJ, 89, 489
- Turner, E.L. 1976, ApJ, 208, 304
- Valtonen, M.J., & Byrd, G.G. 1986, ApJ, 303, 523
- Woods, D.F., Geller, M.J., & Barton, E.J., 2006, AJ, 132, 197